Acta Pharmacologica Sinica (2010) 31: 839–848
 1671-4083/10 $32.00
www.nature.com/aps

Original Article

Leukamenin F suppresses liver fibrogenesis by inhibiting both hepatic stellate cell proliferation and extracellular matrix production

Qiong LIU, Xu WANG, Yu ZHANG, Chen-jing LI, Li-hong HU*, Xu SHEN*

State Key Laboratory of Drug Research, Shanghai Institute of Materia Medica, Chinese Academy of Sciences, Shanghai 201203, China

Aim: To investigate the inhibitory effect of the natural product Leukamenin F on liver fibrosis and explore its potential underlying mechanisms.
Methods: Carbon tetrachloride (CCl_4)-treated mouse model *in vivo* and in hepatic stellate cells (HSC) *in vitro* were used. The effect on CCl_4-induced liver fibrosis was studied using histochemical and biochemical analysis, while the inhibition on HSC was assessed using cell proliferation/apoptosis assay and collagen I production using real-time PCR. The inhibitory effects of Leukamenin F on Akt/mTOR/p70S6K and TGFβ/Smad pathways was studied using Western blot and cell image analysis.
Results: Leukamenin F (0.1–1 mg/kg, ip, q.d.×28) significantly reduced α-SMA and collagen specific Sirius red staining areas in CCl_4 -treated mouse livers. This compound at 1–2 μmol/L dose-dependently inhibited α-SMA expression, cell proliferation and type I procollagen mRNA expression in activated HSC. Furthermore it inhibited the Akt/mTOR/p70S6K pathway and suppressed TGFβ -induced Smad2/Smad3 phosphorylation and nuclear translocation in HSC.
Conclusion: Our results demonstrated that Leukamenin F could attenuate CCl_4-induced liver fibrogenesis in mice as an efficient inhibitor against both HSC proliferation and ECM production. This natural product provides a valuable structural hint for the development of anti-liver fibrosis reagents.

Keywords: Leukamenin F; liver fibrosis; carbon tetrachloride; hepatic stellate cells; Akt; collagen

Acta Pharmacologica Sinica (2010) 31: 839–848; doi: 10.1038/aps.2010.64; published online 21 June 2010

Introduction

Hepatic fibrosis and its endstage cirrhosis, with life-threatening complications of portal hypertension and liver failure, have become major public health problems[1]. Hepatic fibrosis is a wound healing response to chronic liver injury[2] insulted mainly by HCV infection, alcohol abuse and nonalcholic steatohepatitis (NASH)[3]. Hepatic stellate cell (HSC) is a versatile mesenchymal cell, whose activation into the contractile extracellular matrix (ECM)-producing myofibroblast constitutes the major pathway in hepatic fibrosis[4].

The phosphatidylinositol 3-kinase (PI3K)/Akt pathway controls a variety of cellular responses including survival, proliferation and metabolism[5], and is strongly activated in HSC by the potent mitogen PDGF[6]. Akt activates mammalian target of rapamycin (mTOR) through inhibition of TSC2[7], while mTOR, a master regulator of protein synthesis, activates p70 ribosomal protein S6 kinase (p70S6K) which promotes protein translation[8]. Recently, it was reported that inhibition of the mTOR/p70S6K pathway led to reduced type I collagen accumulation and HSC proliferation[9]. These findings have thus implied that suppression of the Akt/mTOR/p70S6K pathway may serve as a promising anti-fibrotic strategy.

As reported, activated HSC is the principal cell type for type I collagen production in response to TGFβ, the most potent factor in stimulating type I collagen gene transcription[10]. The Smad proteins are reported to transduce TGFβ signaling to the nucleus and regulate collagen gene expression[10]. Studies have revealed that blocking the TGFβ/Smad pathway may serve as a promising therapeutic strategy against fibrotic disease[1].

Currently, although varied agents aiming at inhibiting the accumulation of activated HSC and preventing the deposition of ECM are under investigation, few of them are tolerable and effective *in vivo*, while their efficacy and safety in humans are as yet largely unknown[3]. Therefore, the search for the

* To whom correspondence should be addressed.
E-mail xshen@mail.shcnc.ac.cn (Xu SHEN);
simmhulh@mail.shcnc.ac.cn (Li-hong HU).
Received 2009-11-27 Accepted 2010-05-07

efficient anti-liver fibrotic agents has always been an alluring project, and natural products have supplied an abundant resource for this purpose. In fact, many herbal compounds traditionally used in Asian countries have been discovered to exhibit strong antifibrotic efficiency[11]. The *Rabdosia* species are widely used in Chinese folk medicine for the treatment of bacterial infections, inflammation, cancer, etc. Over the past twenty years, they have received considerable attentions in the phytochemical and biological fields[12]. Leukamenin F (Figure 1), one of the major active diterpenoids isolated initially from *Rabdosia japonica*[13], was reported to exhibit anti-tumor activity[14] and inhibit aggregation of platelets[15].

In the present study, we reported the activity and pharmacological mechanisms of Leukamenin F in the treatment of liver fibrosis. Our work demonstrated that this natural product ameliorated the progression of CCl_4-induced liver fibrosis in mice. It could not only inhibit HSC proliferation through the Akt/mTOR/p70S6K pathway but also reduce ECM production through the TGFβ/Smad pathway. The findings were expected to expand the current knowledge of the pharmacological interests for the *Rabdosia* species, while Leukamenin F may further provide structural information as a promising lead compound for the treatment of liver fibrosis.

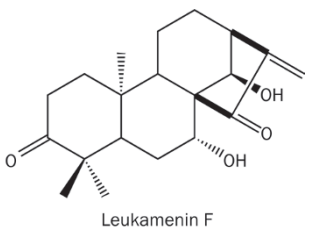

Leukamenin F

Figure 1. Chemical structure of Leukamenin F (Leuk F).

Materials and methods

Materials

The extraction of Leukamenin F was described according to the supplementary method. During the assay, Leukamenin F was dissolved in dimethyl sulfoxide (DMSO) as a 20 mmol/L stock solution and stored at -20 °C. Penicillin-streptomycin, DMEM medium and FBS were obtained from Invitrogen. TGFβ1, SRB (Sulforhodamine B), Sirius red (Direct red 80), and all other chemicals were of analytical grade, and purchased from Sigma-Aldrich.

Animals and treatments

Male C57/BL6 mice (19–22 g) were randomly divided into 5 groups (9 mice for each group). The animals were purchased from SLAC Laboratory Animal Corp (Shanghai, China). All mice were fed with chow diet and kept at 21–25 °C under a 12–h dark/light cycle. The CCl_4-induced liver fibrosis model was set up according to published method[16, 17] with some modifications. The model group bearing CCl_4-induced liver fibrosis was generated by intraperitoneal injection (ip) of 0.5 mL/kg CCl_4 [diluted 1:10 (*v/v*) in olive oil] twice weekly, and injected with the same volume of 5% ethanol diluted in phosphate-buffered saline (PBS) for the other days per week. The control group was administered olive oil twice weekly, and injected with the same volume of PBS for the other days per week. The treatment groups were injected with CCl_4 as the model group and simultaneously ip injected with Leukamenin F (0.1, 0.3, 1 mg/kg) for 4 weeks daily. Leukamenin F was dissolved in Tween-80 as a 100 mg/mL stock solution and diluted to the final concentrations with PBS (containing 1% Tween-80). The control and model groups were ip injected with vehicle (1% Tween-80) daily. 48 h after the last CCl_4 injection, animals were sacrificed after being anesthetized by ip 10% chloral hydrate (5 mL/kg). Liver samples obtained from the lobes were either fixed with 10% formalin or snap frozen with liquid nitrogen and stored at -80 °C until use. Meanwhile, serum was collected and stored at -80 °C for analyzing the activity of alanine aminotransferase (ALT) and aspartate aminotransferase (AST). All procedures in this experiment were performed according to the institutional ethical guidelines on animal care.

Histological studies

Formalin fixed liver specimens were cut into 5 μm sections for histological staining. Thin sections were deparaffinized and stained with hematoxylin and eosin (HE) or Sirius red. For Sirius red staining, the sections were stained for 1 h at room temperature, dehydrated with ethanol and xylene, and mounted. The sections on the slides were examined by light microscopy and red stained collagen fibres were quantified with Image-Pro Plus software (MediaCybernetics, MicroMecanique, France). The fraction of positively stained pixels relative to the total pixels was expressed as percentage of Sirius red staining. Quantitative analysis was calculated from five fields for each liver slice of the nine mice in each group.

Immunohistochemical staining for α-smooth muscle actin (α-SMA) was performed using the avidin-biotin-peroxidase complex method. Antibody for α-SMA and SABC detection kit were purchased from Boster (Wuhan, China). Thin sections were deparaffinezed and treated with 0.3% hydrogen peroxide for 10 min to block endogenous peroxidase activity. The sections were further blocked by 1% bovine serum albumin and were then incubated with primary antibody against α-SMA (1:200) for 1 h at room temperature. After rinsing, the sections were incubated with biotinylated secondary antibody for 20 min at room temperature. α-SMA expression was visualized by diaminobenzidine staining. Quantitative analysis was calculated from five fields for each liver slice of the nine mice in each group using Image-Pro Plus software as described for that of Sirius red staining.

Determination of serum AST and ALT activities

Activities of serum aspartate aminotransferase (AST) and alanine aminotransferase (ALT) were determined using a commercially available kit with the HITACHI 7080 autoanalyzer (Hitachi Inc, Japan).

Cell lines and cell cultures

Primary HSCs were isolated from normal livers of male Sprague-Dawley rats by a 2-step perfusion using pronase E and collagenase D (Sango, China), followed by Nycodenz (Sigma-Aldrich) 2-layer discontinuous density gradient centrifugation as previously described[18]. Purity of rat HSC preparations was assessed by autofluorescence at day 1. HSCs were cultured on uncoated plastic tissue culture dishes in Dulbecco's modified Eagle's medium (DMEM) supplemented with 20% heat inactivated fetal bovine serum (FBS), 100 U/mL penicillin and 100 μg/mL streptomycin (Invitrogen), and maintained in an incubator with a humidified atmosphere of 95% air and 5% CO_2 at 37 °C. Activated HSCs were generated by continuous culture of freshly isolated cells on uncoated plastic dishes for 7−10 days. The fully transdifferentiated rat HSCs between days 10 and 14 were used for experiments.

The human hepatic stellate cell line LX-2 was kindly provided by Dr S L FRIEDMAN (Mount Sinai School of Medicine, New York). As described[19], LX-2 cells were cultured in DMEM supplemented with 10% heat inactivated FBS, 100 U/mL penicillin and 100 μg/mL streptomycin (Invitrogen), and maintained in an incubator with a humidified atmosphere of 95% air and 5% CO_2 at 37 °C. CHO/EGFP-Smad2 cells were purchased from Thermo Scientific (Denmark), and cultured in F-12 medium supplemented with 10% FBS, 100 U/mL penicillin and 100 μg/mL streptomycin.

Cell proliferation assay

The effect of Leukamenin F on cell viability was determined using the sulforhodamine B (SRB) assay as described by Skehan *et al*[20]. Briefly, 1×10^4 cells per well were plated in 96-well plates for 24 h, and then treated with varied concentrations of Leukamenin F (0−20 μmol/L) for 24, 48, and 72 h. Cells were fixed, washed and stained with SRB dye. Unbound dye was removed and the optical density of bound dye was measured at 564 nm using a microplate spectrophotometer (Bio-Rad Laboratories). The effect of Leukamenin F on cell viability was assessed as percent cell viability compared to DMSO-treated control cells, which were arbitrarily assigned 100% viability.

Analysis of apoptotic morphology

Apoptotic morphology was studied by staining the cells with Hoechst 33342 stain. Cells were seeded on coverslips in a 6-well plate in the presence or absence of Leukamenin F (0, 1, and 2 μmol/L). After 24 h incubation, the cover glasses were carefully washed with PBS and stained with 2 μmol/L of Hoechst 33342 for 15 min. Thereafter, the cells were washed in PBS and observed under a fluorescence microscope (Olympus, Germany). Nuclei condensation and fragmentation was considered as apoptotic morphology. The percentage of apoptotic morphology was defined as apoptotic nuclei versus total nuclei numbers in a field. Five fields were taken for each cover-slip, and the experiment was carried out in triplicate.

Flow cytometry assay

To determine the effect of Leukamenin F on the cell cycle, LX-2 cells at 70% confluence were treated with varying concentrations of Leukamenin F (0−2 μmol/L) in complete medium for 24 h, washed, and fixed with 70% ethanol. After an overnight incubation at 4 °C, cells were washed with PBS and incubated with 0.5 mg/mL RNase A at 37 °C for 30 min. The cells were then incubated with 25 μg/mL propidium iodide on ice for 1 h in the dark. The cell cycle distribution of the cells was analyzed using FACS Calibur instrument (BD Biosciences, San Jose, CA) equipped with CellQuest 3.1 software.

Western blot analysis

Cells were lysed with lysis buffer containing 25 mmol/L Tris-HCl (pH 7.5), 150 mmol/L NaCl, 1 mmol/L Na_3VO_4, 1% Triton X-100 and protease cocktails (Sigma-aldrich). Protein concentrations were determined using BCA protein assay kit (Pierce, Rockford, IL). Equal amounts of lysates (30−40 μg of protein) were resolved with 10% sodium dodecyl sulfate polyacrylamide gel electrophoresis (SDS-PAGE). Following electrophoresis, protein blots were transferred to a nitrocellulose membrane and probed with the corresponding primary antibodies. The membrane was then incubated with appropriate horse radish peroxidase (HRP)-conjugated secondary antibodies, and the protein expression was detected by SuperSignal West Dura substrate (Pierce). Antibodies for phospho-Smad2 (Ser465/467), phospho-Smad3 (Ser423/425), Smad2, Smad3, Cyclin D1, Cyclin B1, PARP, phospho-p70S6K (Thr421/Ser424), p70S6K, phospho-mTOR (Ser2448), phospho-Akt (Ser473) and Akt were purchased from Cell Signaling Technology; antibodies for Bcl-2, Bax, and caspase 3 were from Santa Cruz; antibody for cleaved-caspase 3 was from Chemicon; antibody for GAPDH was purchased from KangChen (Shanghai, China). The HRP-conjugated goat anti-rabbit and goat anti-mouse secondary antibodies were purchased from Jackson ImmunoResearch Laboratories (West Grove, USA). The experiments were performed in triplicates and bands were quantified using Image-Pro Plus software and statistically analyzed. Each band was calculated as "intensity×area" using the Image-Pro Plus software (MediaCybernetics). SD was calculated from three repeats of the experiment.

Real-time PCR

LX-2 cells were plated in 6-well plates and cultured to 70% confluence. Cells were pretreated with Leukamenin F (0−2 μmol/L) in serum-free DMEM supplemented with 0.2% BSA, in the absence or presence of 2 ng/mL TGF-β1 for 24 h. Total RNA was extracted with TRIzol reagent (Invitrogen). Complementary DNA was synthesized using PrimeScript™ RT reagent Kit (TaKaRa, Japan). Real-time PCR was performed using SYBR Green Real time PCR master mix (TOYOBO, Japan) on DNA Engine Opticon 2 System (Bio-Rad Laboratories, USA). The primer pairs are: rat α1(I) procollagen: (F) 5′-CAC TCA GCC CTC TGT GCC-3′ and (R) 5′-ACC TTC GCT TCC ATA CTC G-3′; rat α2(I) procollagen: (F) 5′-AGA ATT CCG TGT GGA GGT TG-3′ and (R) 5′-GAG GGA GGG GAC TTA TCT GG-3′. The primer pairs for human α1(I) procollagen, α2(I) procollagen, and rat 18s RNA were

designed as described[19, 21]. The PCR cycle was 95 °C for 10 s, 58 °C for 45 s and 72 °C for 30 s.

Smad2 nuclear translocation assay

Smad2 nuclear translocation assay was performed by using the CHO/EGFP-Smad2 stable cell line. Briefly, CHO/EGFP-Smad2 cells were seeded in 96-well plates and cultured for 24 h. The cells were pretreated with Leukamenin F (0–2 μmol/L) for 10 h, and then treated with TGFβ (2 ng/mL) for 2 h. Finally, the nucleus was stained with 2 μmol/L Hoechst 33342 for 15 min. Images were taken by INCell Analyzer 1000 instrument (GE Healthcare) and data was analyzed with the INCell Analyzer analysis software. Each treatment was repeated in 3 wells and pictures of 5 fields were taken for each well. The ratio of fluorescence intensity in the nuclear and cytoplasm was defined as Nuc/Cyto Smad2 to indicate nuclear location of Smad2. The experiment was repeated for at least twice.

Data analysis

Results are expressed as mean±SD. The statistical difference between multiple treatments and control was analyzed using one way ANOVA, followed with the Dunnett's post test. A P value of less than 0.05 was considered statistically significant.

Results

Leukamenin F attenuated CCl_4-induced liver fibrosis in mice

As reported, prolonged low dose CCl_4 administration induces hepatic fibrogenesis, which largely resembles the hepatic fibrosis in human disease[22]. We thereby constructed the CCl_4-induced mouse hepatic fibrosis model for the current research. In the assay, the effects of Leukamenin F on the liver of CCl_4 administrated mice were initially evaluated by histological analysis. As shown in Figure 2A, compared with the control group, hematoxylin and eosin (HE) staining of the liver sections of the model group showed prominent hepatic steatosis, necrosis, and regenerative nodule and fibrotic septa formation between the nodules as indicated by arrows. Leukamenin F administration (0.1–1 mg/kg) precluded the steatosis progression and fibrogenesis as indicated by attenuated vesicular steatosis and reduced thickness of bridging fibrotic septa.

To further assess the protective effect of Leukamenin F on liver fibrogenesis, Sirius red staining, a collagen specific staining method was used to quantify collagen depositions. As indicated in Figure 2B, liver sections of the model group showed prominent red staining compared with the control group. Leukamenin F treatment (0.1−1 mg/kg) reduced Sirius red stained area in comparison with the model group (P<0.01–0.001) as quantified by the Image-Pro Plus software (Figure 2D).

As the unique marker of activated HSC, α-SMA was stained immunohistochemically to investigate the cellular events in mice. Compared with the control group, which showed scarce staining, the model group was extensively (P<0.001) stained (Figure 2C), indicating that HSC was activated in the CCl_4-treated mouse model. However, an obvious decrease was discovered for α-SMA staining in Leukamenin F-treated group at the dose of 1 mg/kg compared with the model group (Figure 2E, P<0.05). Additionally, Leukamenin F (1 mg/kg) dramatically decreased CCl_4-induced serum AST (Figure 3A, P<0.5) and ALT (Figure 3B, P<0.01) activities with dose-dependency, although high doses of Leukamenin F failed to exert these effects (Figure S2).

Taken together, Leukamenin F attenuated CCl_4-induced liver fibrosis in mice.

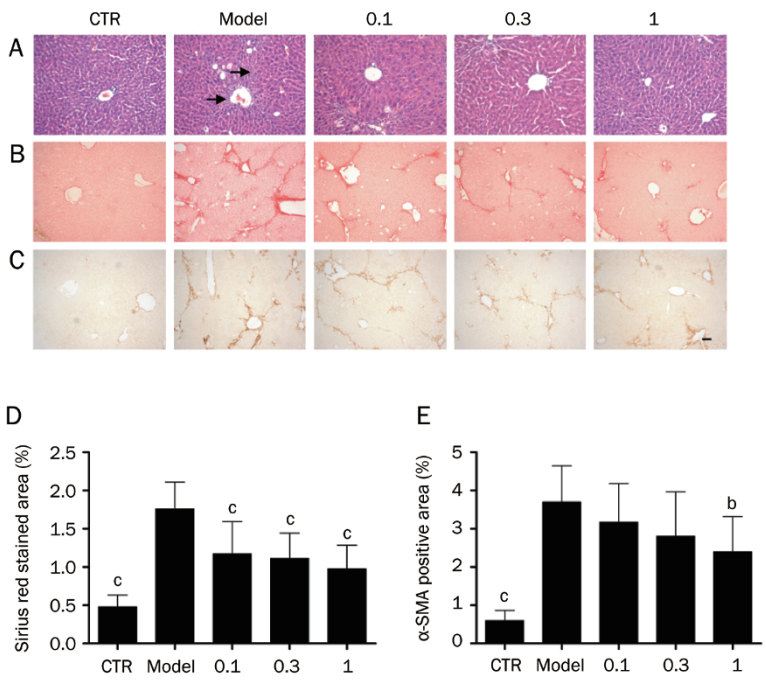

Figure 2. Leukamenin F protects the liver against CCl_4-induced hepatic fibrosis in mice. Mice were induced with CCl_4 (Model group) or vehicle (CTR group) and model mice were treated with 0.1, 0.3, and 1 mg/kg Leukamenin F (groups 0.1, 0.3, and 1). Representative views of liver slices from each group (n=9) stained with hematoxylin and eosin (HE) (A), Sirius red (B) and immunohistochemically stained with antibody against α-SMA (C) are presented (scale bar=50 μm). Sites of fibrotic changes in HE staining are indicated by arrows. Quantitative analysis of B and C is performed (D and E). n=9. ^bP<0.05, ^cP<0.01 compared with the Model group.

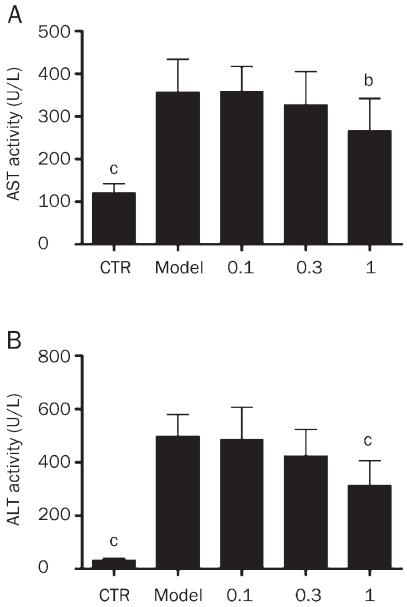

Figure 3. Leukamenin F decreases CCl_4 induced serum AST and ALT activities. Mice were induced with CCl_4 (Model group) or vehicle (CTR group) and model mice were treated with 0.1, 0.3, and 1 mg/kg Leukamenin F (groups 0.1, 0.3, and 1). Serum from mice in each group (n=9) was collected and activities of AST (A) and ALT (B) were analyzed. n=9. ^bP<0.05, ^cP<0.01 compared with the Model group.

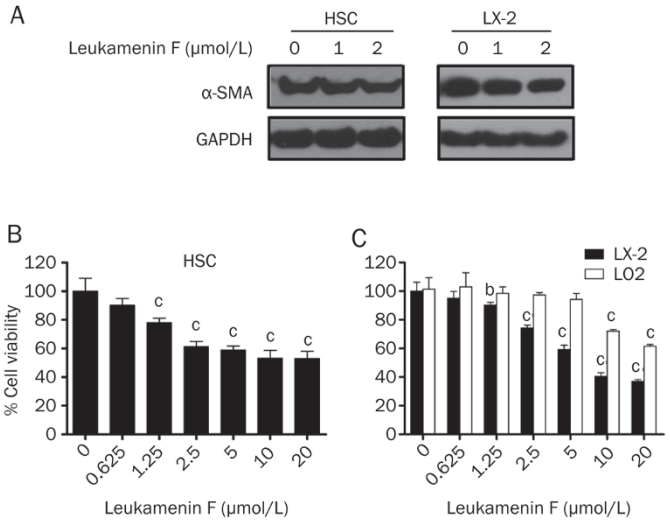

Figure 4. Leukamenin F suppresses HSC activation and proliferation. (a) Leukamenin F suppresses α-SMA expression. Primary rat HSC and LX-2 human hepatic stellate cell were treated with indicated concentrations of Leukamenin F (0−2 μmol/L) for 24 h, expression of α-SMA was determined by Western blotting. GAPDH was used as a loading control. The results shown are representative of three independent experiments. Primary rat HSC (b), LX-2 cell and LO2 hepatocyte (c) were treated with a series of concentrations (0−20 μmol/L) of Leukamenin F for 48 h, and cell viability was determined using SRB assay. n=3. ^bP<0.05, ^cP<0.01 compared with DMSO treated cells (0 μmol/L).

Leukamenin F suppressed HSC activation and proliferation

Activation and proliferation of hepatic stellate cells play pivotal roles in liver fibrosis progression. To explore the potential mechanism responsible for the attenuation of CCl_4-induced liver fibrosis by Leukamenin F, we isolated rat primary HSCs and performed the relevant studies. The results showed that Leukamenin F treatment (0–2 μmol/L, 24 h) dose-dependently reduced α-SMA levels in culture activated HSC (Figure 4A, left panel). In addition, the effect of Leukamenin F on HSC proliferation was determined using SRB assay. The results demonstrated that Leukamenin F treatment (0.625–20 μmol/L) for 48 h (as well as 24 and 72 h, data not shown) dramatically reduced rat primary HSC viability (P<0.001) in a dose-dependent manner (Figure 4B).

To further investigate the inhibition feature of Leukamenin F on hepatic stellate cells in vitro, human hepatic stellate cell line LX-2 was also applied. Similar to that of primary HSC, Leukamenin F treatment (0–2 μmol/L, 24 h) dose-dependently decreased α-SMA level in LX-2 cells (Figure 4A, right panel). The SRB assay showed that Leukamenin F (0–20 μmol/L, 48 h) dramatically (P<0.5–0.001) reduced LX-2 viability (Figure 4C). In contrast to LX-2 cells, normal human hepatocytes (LO2 cells) were resistant to the cytotoxic effects of Leukamenin F, with a marked effect on cell death (P<0.001) observed only at the maximum concentrations (10 and 20 μmol/L) after 48 h treatment (Figure 4C), which was almost 50% less than the effects of the same dose of Leukamenin F on LX-2 cells. Similar results were observed after 24 h and 72 h treatment (data not shown). Thus Leukamenin F appears to be capable of inducing cytotoxic effects on human hepatic stellate cells without incurring apparent cytotoxic effects on normal human hepatocytes.

Leukamenin F induced S-phase arrest in HSC

Since Leukamenin F has been discovered to strongly inhibit HSC, we thereby explored the possible mechanism for its anti-proliferative ability. During the assay, the effect of Leukamenin F on cell cycle progression in LX-2 cells was determined following 24 h of Leukamenin F treatment (0–2 μmol/L) using flow cytometry. As indicated in Figure 5A, Leukamenin F treatment of LX-2 cells caused a dose-dependent increase of S phase cells and a corresponding decrease of G_1 phase cells with minimal change in G_2-M cell population, compared with the DMSO-treated control cells.

As the treatment of LX-2 cells with Leukamenin F induced S phase arrest, we then assessed the effect of Leukamenin F (2 μmol/L) on cell cycle regulatory proteins after different time periods (0–24 h). Cyclin D1, which controls G_1-S transition, was initially induced by Leukamenin F treatment and subsequently decreased after 12 h of treatment, while cyclin B1, the G_2-phase cyclin, was continuously decreased after Leukamenin F treatment (Figure 5B). These results suggested that Leukamenin F may initially promote entry into S phase through upregulation of cyclin D1, and there seems to be a negative feed back response that subsequently decreased cyclin D1 level. However, progression to G_2 phase was

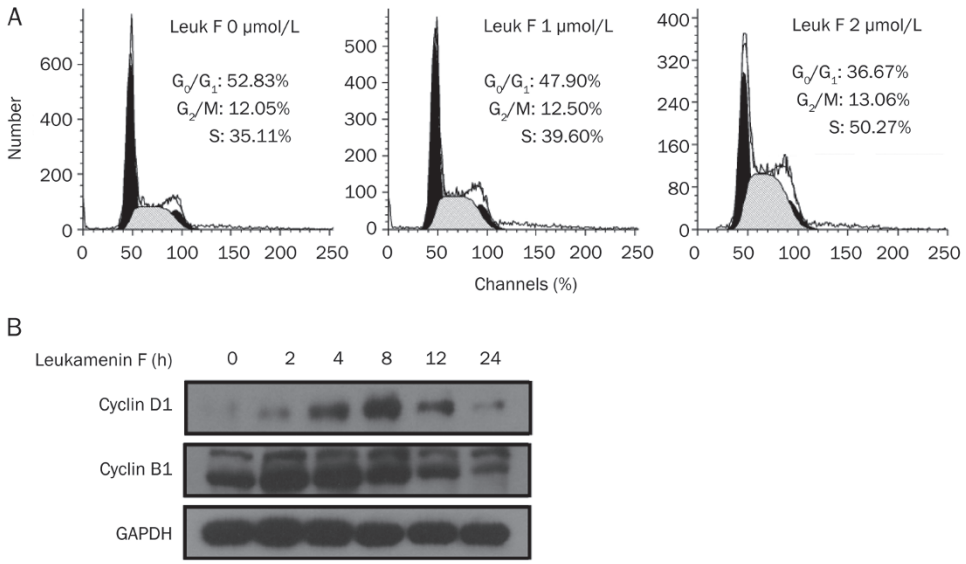

Figure 5. Leukamenin F induces S-phase arrest. (A) Leukamenin F arrests the cells at S phase of cell cycle. LX-2 cells were incubated with indicated concentrations of Leukamenin F (0−2 μmol/L) for 24 h. The cells were fixed, stained with propidium iodide, and analyzed for DNA content by flow cytometry as detailed in Methods. (B) Leukamenin F modulates cell cycle regulatory proteins. LX-2 cells were incubated with 2 μmol/L Leukamenin F for the indicated time points (0−24 h). The cells were harvested and cell lysates were subjected to Western blot analysis to determine cyclin D1 and cyclin B1 levels. GAPDH was used as a loading control. The results shown are representative of three independent experiments.

hindered by reduction of cyclin B1, and the cells were therefore blocked in S phase.

Leukamenin F induced apoptosis in HSC

Since the decrease of cell viability might be due to the decreased cell proliferation or induction of apoptosis, to determine whether the viability loss of Leukamenin F-treated LX-2 cells (Figure 4B) was also attributable to the induction of apoptosis, we examined the morphological changes with Hoechst33342 staining. As shown in Figure 6A, the nuclei were round and homogeneously stained with Hoechst33342 in the control cells, while Leukamenin F treatment (1 and 2 μmol/L, 24 h) dose-dependently induced nuclei condensation and fragmentation in LX-2 cells (indicated by the arrows). Quantitative analysis of the apoptotic morphology (Figure 6B) showed that Leukamenin F induced apoptosis in LX-2 cells at both concentrations used (P<0.01 for 1 μmol/L and P<0.001 for 2 μmol/L).

To further investigate the possible mechanism of Leukamenin F induced apoptosis in LX-2 cells, we examined the expression of apoptotic proteins 24 h after Leukamenin F treatment (Figure 6C), when Leukamenin F induced maximum apoptosis but limited cell death. As reported, the bcl-2 family proteins mediate cell apoptosis mainly through the mitochondria pathway[23], we thus determined the protein levels of bcl-2 and bax. Leukamenin F treatment dose-dependently decreased the anti-apoptotic protein bcl-2 level while increased the pro-apoptotic protein bax. Mitochondrial release of cytochrome c activates caspase 3, followed by the subsequent cleavage of poly (ADP-ribose) polymerase (PARP) and other cellular targets, finally leading to apoptosis[24]. It is discovered that cleaved-caspase 3 was slightly increased, corresponding to a decrease of full length caspase 3 levels after Leukamenin F treatment. Interestingly, Leukamenin F dose-dependently decreased total PARP levels with a concomitant

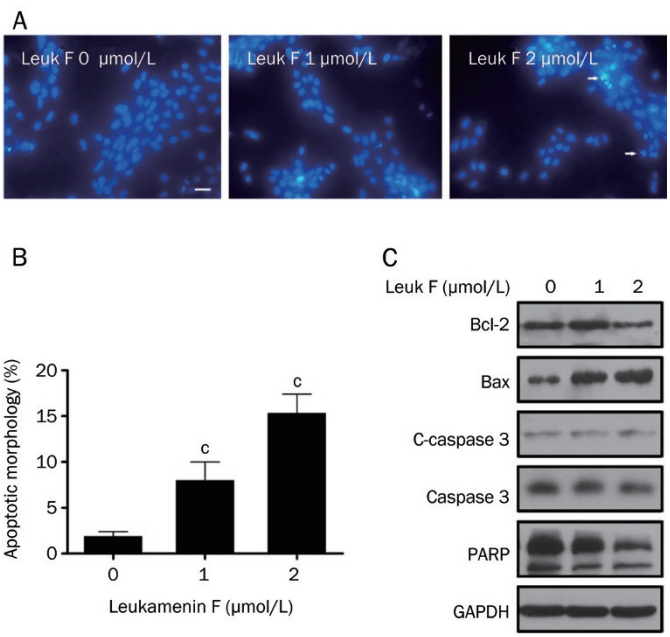

Figure 6. Leukamenin F induces apoptosis. (A) Leukamenin F induces apoptotic morphology in LX-2 cells. LX-2 cells were treated with indicated concentrations of Leukamenin F (0−2 μmol/L) for 24 h. The cells were fixed, stained with Hoechst 33342, and visualized with a fluorescence microscope (Scale bar=50 μm). Representative views from five fields for each slide are shown; the treatments are performed in triplicates. (B) Cells with nuclei condensation and fragmentation (indicated by arrows) were counted and apoptotic morphology was quantified. (C) Leukamenin F regulates apoptotic proteins. LX-2 cells were treated with indicated concentrations of Leukamenin F (0−2 μmol/L) for 24 h. The cells were harvested and cell lysates were subjected to Western blot analysis for the expression of bcl-2, bax, cleaved-caspase 3 (c-caspase 3), and PARP. GAPDH was used as a loading control. The results shown are representative of three independent experiments. n=3. ^{c}P<0.01 compared with DMSO treated (0 μmol/L) control cells.

decrease of the cleaved form. The slight changes of caspase 3 and obvious effects on other apoptotic proteins thus suggested that Leukamenin F may affect the mitochondria pathway and subsequent targets beside the caspase cascade to induce apoptosis in LX-2 cells.

Leukamenin F inhibited procollagen I expression in HSC

Since type I collagen is the major ECM component in fibrotic liver[25], we thereby determined α1/α2 procollagen I mRNA levels by real-time PCR analysis in primary HSC (Figure 7A and 7B) to evaluate the effect of Leukamenin F on ECM production. As indicated, α1 and α2 procollagen I levels were obvious (P<0.001) upregulated by TGFβ stimulation (2 ng/mL) compared with the control group, while decreased almost to the basal level (P<0.001) after Leukamenin F (0–2 μmol/L, 24 h) treatment in comparison with the TGFβ stimulated group. In addition, basal level expression of α1 procollagen I was also inhibited by Leukamenin F treatment, and basal expression of α2 procollagen I was almost unaffected.

Similar to rat primary hepatic stellate cells, LX-2 cell expressed high levels of ECM component proteins including procollagen I upon TGFβ stimulation. Leukamenin F exhibited similar inhibitory effect on procollagen I expression in LX-2 cell as that in primary HSC (Figure 7C and 7D).

Leukamenin F suppressed Akt pathway

Akt pathway promotes cellular proliferation and collagen gene expression in HSC[26], we examined the potential influence of Leukamenin F on Akt activation. Leukamenin F treatment (1–2 μmol/L, 24 h) dose-dependently decreased Akt phosphorylation at Serine 473, without affecting Akt protein levels. Subsequently, we investigated the effect of Leukamenin F on the proteins downstream of Akt (Figure 8). Leukamenin F suppressed mTOR phosphorylation at Serine 2448, a reported Akt phosphorylation site[7], and suppressed the mTOR substrate p70S6 kinse phosphorylation at Threonine 421/Serine 424, phosphorylation of which was thought to activate p70S6K[27]. Since Leukamenin F had no effect on the total proteins of Akt and p70S6K, which are upstream and downstream of mTOR, it is thus expected that this compounds was not likely to affect the total protein of mTOR. Similar results have been also published elsewhere[28–30].

Leukamenin F suppressed TGFβ stimulated Smad2/3 phosphorylation and nuclear translocation

Considering the fact that TGFβ/Smad pathway plays critical role in TGFβ stimulated collagen gene expression, we thereby examined the phosphorylation features of the Smad proteins to further investigate the mechanism for the inhibition of TGFβ stimulated type I collagen gene expression by Leukamenin F.

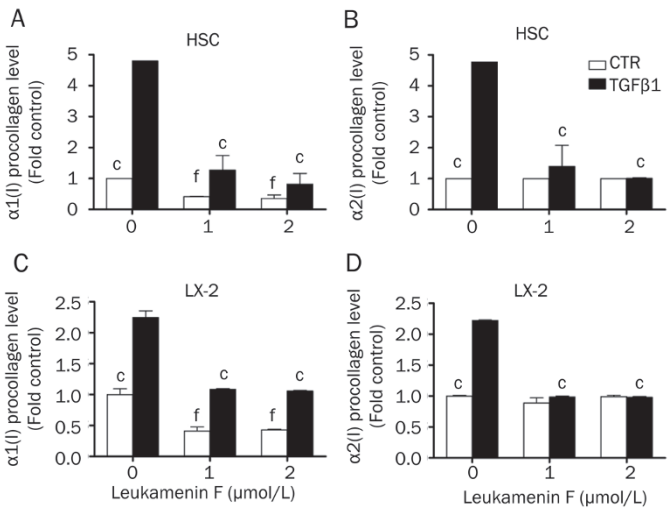

Figure 7. Leukamenin F inhibits procollagen I mRNA expression. Primary rat HSC was treated with indicated concentrations of Leukamenin F (0−2 μmol/L) in the absence or presence of TGFβ (2 ng/mL) for 24 h in DMEM supplemented with 0.2% BSA. mRNA levels of (A) α1 procollagen I and (B) α2 procollagen I were analyzed by real-time PCR assays. Ribosomal 18s RNA was used as an internal control for calculating mRNA fold changes. (C) α1 procollagen I and (D) α2 procollagen I of LX-2 cells were analyzed as that of primary HSC. ^{c}P<0.01 compared with DMSO (0 μmol/L) and TGFβ treated cells. ^{f}P<0.01 compared with DMSO (0 μmol/L) treated control cells.

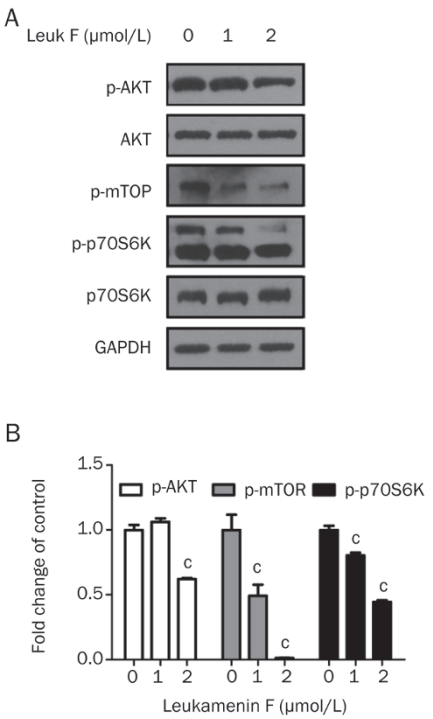

Figure 8. Leukamenin F inhibits Akt pathway. (A) Primary rat HSC was incubated with indicated concentrations of Leukamenin F (0−2 μmol/L) for 24 h. The cells were harvested and subjected to Western blot analysis for phosphorylated Akt (Ser 473), Akt, phosphorylated mTOR (Ser 2448), phosphorylated p70S6K (Thr 421/Ser 424), and p70S6K. GAPDH was used as a loading control. The results shown are representative of three independent experiments. (B) The bands were quantified using Image-Pro Plus software. ^{c}P<0.01 compared with control cells.

As shown in Figure 9A, TGFβ (2 ng/mL) potently upregulated Smad2 and Smad3 phosphorylation, Leukamenin F treatment (0–2 μmol/L, 24 h) efficiently inhibited TGFβ induced Smad2 phosphorylation, without affecting Smad2 protein levels. However, TGFβ stimulated phosphorylation of Smad3 was only slightly decreased by Leukamenin F treatment, without changes in Smad3 protein levels.

Phosphorylated Smad proteins translocate to the nucleus to regulate collagen gene transcription, therefore we also assessed whether Leukamenin F could block TGFβ stimulated Smad2 translocation. As shown in Figure 9B, the majority of EGFP-Smad2 protein localized in the cytoplasm in unstimulated cells and translocated to the nucleus upon TGFβ stimulation. While Leukamenin F dose-dependently blocked TGFβ stimulated Smad2 nuclear translocation, which was quantified in Figure 9C ($P<0.01$).

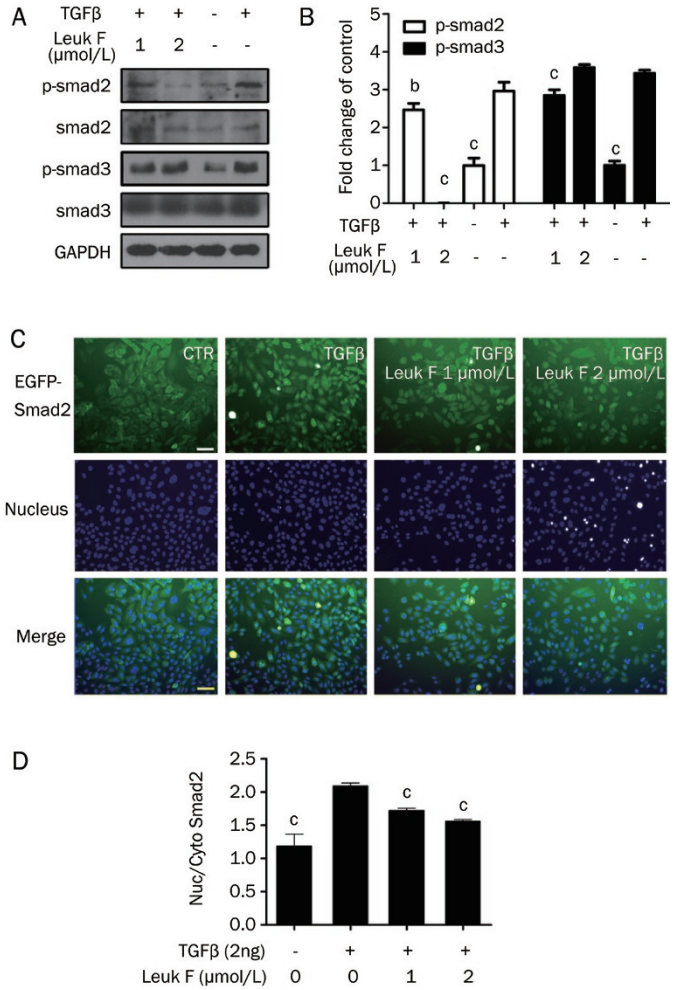

Figure 9. Leukamenin F inhibits TGFβ stimulated Smad2/3 phosphorylation and nuclear translocation. (A) Leukamenin F inhibits TGFβ stimulated Smad2/3 phosphorylation. Primary rat HSC was treated with indicated concentrations of Leukamenin F (0−2 μmol/L) in the absence or presence of TGFβ (2 ng/mL) for 24 h in DMEM supplemented with 0.2% BSA. The cells were harvested and subjected to Western blot analysis for phosphorylated Smad2 (Ser 465/467), Smad2, phosphorylated Smad3 (Ser 432/425), and Smad3. GAPDH was used as a loading control. The results shown are representative of three independent experiments. (B) The bands were quantified using Image-Pro Plus software. (C, D) Leukamenin F inhibits TGFβ stimulated Smad2 nuclear translocation. CHO/EGFP-Smad2 cells were pretreated with Leukamenin F (0, 1, and 2 μmol/L) for 10 h, and then stimulated with TGFβ (2 ng/mL) for 2h in serum free F-12 medium supplemented with 0.2% BSA. Cells were stained with 2 μmol/L hoechst 33342 for 15 min and images were taken by INCell Analyzer 1000. Each treatment was repeated in 3 wells and 5 fields for each well were photographed. (c) Representative views are shown (scale bar=50 μm) and (d) data was quantified using the INCell Analyzer analysis software. $^{b}P<0.05$, $^{c}P<0.01$ compared with TGFβ stimulated cells.

Discussion

The *Rabdosia* speices has long been used in traditional Chinese medicine, with diterpenoids as the major biological active components[12]. Here, we reported that Leukamenin F, a diterpenoid extracted from the *Rabdosia* species, could efficiently ameliorate CCl_4 induced liver fibrosis in mice. Further research suggested that this natural product may exert its anti-fibrotic role through inhibition of HSC proliferation and ECM production, involving the AKT/mTOR/p70S6K and TGFβ/Smad pathways (Figure 10).

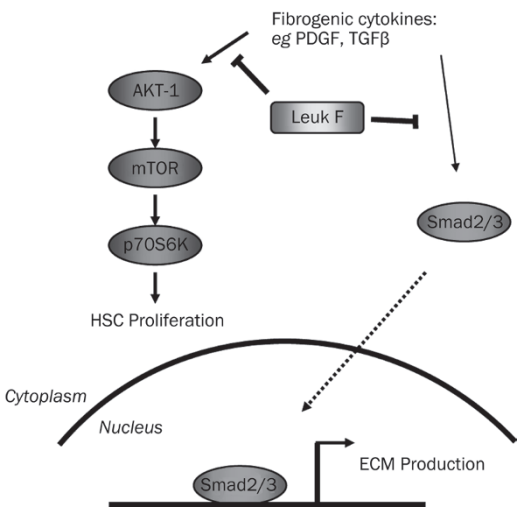

Figure 10. Proposed model illustrating the anti-fibrotic mechanism of Leukamenin F. During liver fibrosis, stimulatory signals from the fibrogenic cytokines including PDGF and TGFβ are transduced to into the cells through their corresponding receptors, which in turn activate the Akt and Smad proteins by phosphorylation. Leukamenin F inhibited the phosphorylation of Akt and its down stream targets mTOR and p70S6K, and finally led to reduced HSC proliferation. Meanwhile, Leukamenin F suppressed Smad2/3 phosphorylation and therefore blocked their translocation into the nucleus, thus resulted in reduced transcription of ECM proteins.

To our knowledge, most of the published natural compounds exhibited liver-protecting activities at high doses. For example, curcumin decreased CCl_4-induced AST and ALT activity by 36% at 200 mg/kg[16]. Another well-known natural product berberine was reported to decrease CCl_4-induced AST

and ALT activity by about 30% at 200 mg/kg[31]. Leukamenin F in our study could decrease AST and ALT activities (by around 30%) at very low dose (1 mg/kg), suggesting that Leukamenin F might be a potent liver-protective natural product for further research. Besides, according to theoretical correlation, 2 μmol/L in the cellular assay is equivalent to about 1 mg/kg in animal studies.

The isolation and culture of rodent primary HSC[32] and establishment of human hepatic stellate cell line[19] have greatly facilitated researches on liver fibrosis. In our work, Leukamenin F showed strong inhibition against the activation marker α-SMA, the cell viability and collagen I expression in both rat primary HSC and human LX-2 cell line, thus implying that this compound might find its potential application in both rodents and man, although the regulation of HSC activation and α-SMA expression is quite complicated and further investigations are required.

Inhibition of proliferation and induction of apoptosis in HSC are both effective ways to clear activated HSC[25]. Our work demonstrated Leukamenin F reduced HSC viability by inhibition of cell proliferation and induction of apoptosis. Further studies indicated that the anti-proliferative activity of Leukamenin F was possibly due to S phase arrest through dynamic regulation of Cyclin D1 and Cylin B1. Beside inhibition of HSC proliferation, Leukamenin F also induced LX-2 cell apoptosis, as indicated by the induction of apoptotic morphology and apoptotic proteins. These results suggested that Leukamenin F may potently reduce the number of activated HSC, which is also evidenced by reduced α-SMA staining *in vivo*.

The PI3K-Akt signaling pathway promotes cell proliferation and collagen gene expression in HSC. PI3K inhibition suppresses cell proliferation and type I collagen gene expression in activated HSC[26]. p70S6K regulates protein synthesis and proliferation, blocking of its upstream kinase mTOR inhibited DNA synthesis and cyclin D1 expression in HSC[9]. Besides, the Akt pathway also promotes cell survival by inhibition of apoptosis[33]. Our work showed that Leukamenin F decreased Akt, mTOR and p70S6K phosphorylation levels, indicating that the Akt/mTOR/p70S6K signaling pathway may at least partially account for the inhibitory effect of Leukamenin F on HSC proliferation and survival.

The accumulation of ECM proteins distorts the hepatic architecture by forming a fibrous scar, and the subsequent development of nodules of regenerating hepatocytes defines cirrhosis[34]. Our work showed that Leukamenin F reduced TGFβ stimulated α1 and α2 procollagen I mRNA expression in both rat primary HSC and LX-2 human hepatic stellate cells. What's more, Leukamenin F reduced collagen specific Sirius red staining in CCl_4-treated mouse livers, which may contribute to the improved liver architecture as analyzed by HE staining. These results demonstrated that Leukamenin F could potently inhibit both collagen α1 and α2 chain expressions, thus ameliorate liver fibrosis *in vivo*. Upon TGFβ stimulation, the receptor kinase TGFβ-R1 phosphorylates Smad2 (Ser465/467) and Smad3 (Ser423/425) at their carboxy-termini. Phosphorylated Smad2 and Smad3 form a heteromeric complex with the co-Smad and then translocate to the nucleus to bind DNA and regulate gene transcription[35]. Our results demonstrated that Leukamenin F inhibited TGFβ stimulated Smad2/3 phosphorylation and Smad2 nuclear translocation, therefore, inhibition of TGFβ-induced α2(I) procollagen expression by Leukamenin F was likely due to impaired transcriptional machinery. Leukamenin F exerts slight effects on Smad3 compared with Smad2. This differential regulation might be due to the difference in phosphorylation sites of Smad2 and Smad3. Since Smad2 is an essential regulator that translocates to nucleus in response to TGFβ, our results might implicate that Leukamenin F mainly affects Smad2 phosphorylation to block TGFβ signaling. While TGFβ stimulated COL1A1 gene expression is reported to be regulated through a hydrogen peroxide and C/EBPβ dependent mechanism[36], our work showed that Leukamenin F did not affect TGFβ-induced hydrogen peroxide as analyzed by the DCFH-DA fluorescein probe as indicated in Figure S1. Therefore, Leukamenin F may inhibit TGFβ-induced α1(I) procollagen transcription through other mechanisms. Besides, Leukamenin F decreased basal level α1(I) procollagen mRNA expression but not that of α2(I) procollagen, which may be attributable to differential regulation of basal COL1A1 and COL1A2 genes. Inhibition of basal level α1(I) procollagen mRNA by Leukamenin F may be attributable to decreased Akt activity, as reported by Reif *et al*[26].

In conclusion, the present study provides evidence that Leukamenin F, a diterpenoid extracted from the *Rabdosia* species, protected mouse liver from CCl_4-induced liver fibrosis through inhibition of HSC proliferation and ECM production. The obtained results have further provided additional understandings on the biological activities and underlying mechanisms of the *Rabdosia* species.

Acknowledgements

We thank Dr SL FRIEDMAN (Mount Sinai School of Medicine, New York) for kindly providing the human stellate cell line LX-2. This work was supported by the State Key Program of Basic Research of China (grants 2010CB912501, 2007CB914304), the National Natural Science Foundation of China (grants 30890044, 20721003), and Key New Drug Creation and Manufacturing Program (2009ZX09301-001).

Author contribution

Qiong LIU performed the research; Xu WANG helped the animal experiments; Yu ZHANG helped data interpretation; Chen-jing LI helped animal administration; Li-hong HU and Xu SHEN supervised the project.

Supplementary information is available at Acta Pharmacologica Sinica website of NPG.

References

1 Lotersztajn S, Julien B, Teixeira-Clerc F, Grenard P, Mallat A. Hepatic fibrosis: molecular mechanisms and drug targets. Annu Rev Pharmacol Toxicol 2005; 45: 605–28.

2 Albanis E, Friedman SL. Hepatic fibrosis. Pathogenesis and principles

of therapy. Clin Liver Dis 2001; 5: 315–34, v–vi.
3 Bataller R, Brenner DA. Liver fibrosis. J Clin Invest 2005; 115: 209–18.
4 Friedman SL. Molecular regulation of hepatic fibrosis, an integrated cellular response to tissue injury. J Biol Chem 2000; 275: 2247–50.
5 Scheid MP, Woodgett JR. PKB/AKT: functional insights from genetic models. Nat Rev Mol Cell Biol 2001; 2: 760–8.
6 Marra F, Gentilini A, Pinzani M, Choudhury GG, Parola M, Herbst H, *et al*. Phosphatidylinositol 3-kinase is required for platelet-derived growth factor's actions on hepatic stellate cells. Gastroenterology 1997; 112: 1297–306.
7 Memmott RM, Dennis PA. Akt-dependent and -independent mechanisms of mTOR regulation in cancer. Cell Signal 2009; 21: 656–64.
8 Sarbassov DD, Ali SM, Sengupta S, Sheen JH, Hsu PP, Bagley AF, *et al*. Prolonged rapamycin treatment inhibits mTORC2 assembly and Akt/PKB. Mol Cell 2006; 22: 159–68.
9 Gabele E, Reif S, Tsukada S, Bataller R, Yata Y, Morris T, *et al*. The role of p70S6K in hepatic stellate cell collagen gene expression and cell proliferation. J Biol Chem 2005; 280: 13374–82.
10 Inagaki Y, Okazaki I. Emerging insights into transforming growth factor beta Smad signal in hepatic fibrogenesis. Gut 2007; 56: 284–92.
11 Shimizu I. Sho-saiko-to: Japanese herbal medicine for protection against hepatic fibrosis and carcinoma. J Gastroenterol Hepatol 2000; 15 Suppl: D84–90.
12 Sun HD, Huang SX, Han QB. Diterpenoids from Isodon species and their biological activities. Nat Prod Rep 2006; 23: 673–98.
13 Xu YL, Sun XC, Sun HD, Lin ZW, Wang DZ. Chemical structures of glaucocalyxin A and B. Acta Botan Yunnan 1981; 3: 283–6.
14 Zhao Y, Huang SX, Yang LB, Pu JX, Xiao WL, Li LM, *et al*. Cytotoxic ent-kaurane diterpenoids from *Isodon henryi*. Planta Med 2009; 75: 65–9.
15 Bin Z, Kun L. Inhibition by glaucocalyxin A of aggregation of rabbit platelets induced by ADP, arachidonic acid and platelet–activating factor, and inhibition of [^{3}H]–PAF binding. Thromb Haemost 1992; 67: 458–60.
16 Fu Y, Zheng S, Lin J, Ryerse J, Chen A. Curcumin protects the rat liver from CCl_4-caused injury and fibrogenesis by attenuating oxidative stress and suppressing inflammation. Mol Pharmacol 2008; 73: 399–409.
17 Teixeira-Clerc F, Julien B, Grenard P, Tran Van Nhieu J, Deveaux V, Li L, *et al*. CB1 cannabinoid receptor antagonism: a new strategy for the treatment of liver fibrosis. Nat Med 2006; 12: 671–6.
18 Siegmund SV, Uchinami H, Osawa Y, Brenner DA, Schwabe RF. Anandamide induces necrosis in primary hepatic stellate cells. Hepatology 2005; 41: 1085–95.
19 Xu L, Hui AY, Albanis E, Arthur MJ, O'Byrne SM, Blaner WS, *et al*. Human hepatic stellate cell lines, LX-1 and LX-2: new tools for analysis of hepatic fibrosis. Gut 2005; 54: 142–51.
20 Skehan P, Storeng R, Scudiero D, Monks A, McMahon J, Vistica D, *et al*. New colorimetric cytotoxicity assay for anticancer-drug screening. J Natl Cancer Inst 1990; 82: 1107–12.
21 Jinnin M, Ihn H, Tamaki K. Characterization of SIS3, a novel specific inhibitor of Smad3, and its effect on transforming growth factor-beta1-induced extracellular matrix expression. Mol Pharmacol 2006; 69: 597–607.
22 Perez Tamayo R. Is cirrhosis of the liver experimentally produced by CCl_4 and adequate model of human cirrhosis? Hepatology 1983; 3: 112–20.
23 Chao DT, Korsmeyer SJ. BCL-2 family: regulators of cell death. Annu Rev Immunol 1998; 16: 395–419.
24 Thornberry NA, Lazebnik Y. Caspases: enemies within. Science 1998; 281: 1312–6.
25 Friedman SL. Mechanisms of hepatic fibrogenesis. Gastroenterology 2008; 134: 1655–69.
26 Reif S, Lang A, Lindquist JN, Yata Y, Gabele E, Scanga A, *et al*. The role of focal adhesion kinase-phosphatidylinositol 3-kinase-Akt signaling in hepatic stellate cell proliferation and type I collagen expression. J Biol Chem 2003; 278: 8083–90.
27 Pullen N, Thomas G. The modular phosphorylation and activation of p70s6k. FEBS Lett 1997; 410: 78–82.
28 Altomare DA, Wang HQ, Skele KL, De Rienzo A, Klein-Szanto AJ, Godwin AK, *et al*. AKT and mTOR phosphorylation is frequently detected in ovarian cancer and can be targeted to disrupt ovarian tumor cell growth. Oncogene 2004; 23: 5853–7.
29 Stuart CA, Howell ME, Baker JD, Dykes RJ, Duffourc MM, Ramsey MW, *et al*. Cycle training increased GLUT4 and activation of mammalian target of rapamycin in fast twitch muscle fibers. Med Sci Sports Exerc 2010; 42: 96–106.
30 Darb-Esfahani S, Faggad A, Noske A, Weichert W, Buckendahl AC, Muller B, *et al*. Phospho-mTOR and phospho-4EBP1 in endometrial adenocarcinoma: association with stage and grade *in vivo* and link with response to rapamycin treatment *in vitro*. J Cancer Res Clin Oncol 2009; 135: 933–41.
31 Sun X, Zhang X, Hu H, Lu Y, Chen J, Yasuda K, *et al*. Berberine inhibits hepatic stellate cell proliferation and prevents experimental liver fibrosis. Biol Pharm Bull 2009; 32: 1533–7.
32 Friedman SL, Roll FJ, Boyles J, Arenson DM, Bissell DM. Maintenance of differentiated phenotype of cultured rat hepatic lipocytes by basement membrane matrix. J Biol Chem 1989; 264: 10756–62.
33 Fayard E, Tintignac LA, Baudry A, Hemmings BA. Protein kinase B/Akt at a glance. J Cell Sci 2005; 118: 5675–8.
34 Gines P, Cardenas A, Arroyo V, Rodes J. Management of cirrhosis and ascites. N Engl J Med 2004; 350: 1646–54.
35 Abdollah S, Macias-Silva M, Tsukazaki T, Hayashi H, Attisano L, Wrana JL. TbetaRI phosphorylation of Smad2 on Ser465 and Ser467 is required for Smad2-Smad4 complex formation and signaling. J Biol Chem 1997; 272: 27678–85.
36 Garcia-Trevijano ER, Iraburu MJ, Fontana L, Dominguez-Rosales JA, Auster A, Covarrubias-Pinedo A, *et al*. Transforming growth factor beta1 induces the expression of alpha1(I) procollagen mRNA by a hydrogen peroxide-C/EBPbeta-dependent mechanism in rat hepatic stellate cells. Hepatology 1999; 29: 960–70.